ADMET & DMPK **14** (2026) 3512*; doi: https://doi.org/10.5599/admet.3512*

ADMET
Open Access : ISSN : 1848-7718
http://www.pub.iapchem.org/ojs/index.php/admet

Original scientific paper

Inhibition of the mitochondrial fission dynamin-related protein-1 attenuates insulin resistance in hepatoma cells: Implication of mitochondrial dysfunction, apoptosis and nucleolar disruption

Mai H. Hassan, Thoria Donia and Mohamed Hessien*

MCB Unit, Division of Biochemistry, Chemistry Department, Faculty of Science, Tanta University, Tanta, 31527, Egypt

Corresponding Author: E-mail: *mohamed.hussien1@science.tanta.edu.eg; Tel: +1-01069417676

Received: June 17, 2026; Revised: August 13, 2026; Published: August 20, 2026

Abstract

Background and purpose: Chronic hyperglycaemia, a defining feature of diabetes mellitus, is closely associated with excessive mitochondrial fragmentation. Accordingly, inhibition of mitochondrial fission has been proposed as a potential strategy for alleviating insulin resistance; however, the associated mitochondrial, cellular, and nuclear consequences remain insufficiently characterised. **Experimental approach:** In the present study, an insulin-resistant (IR) cellular model was established in HepG2 cells and treated with the mitochondrial division inhibitor (Mdivi-1), a selective inhibitor of dynamin-related protein-1 (DRP1). **Key results:** Exposure of cells to high-glucose medium (25 mM) and insulin (1 nM) decreased glucose uptake, enhanced reactive oxygen species (ROS) production, and downregulated insulin receptor substrate 1 (IRS-1). Also, Mdivi-1 treatment suppressed DRP1 expression in both Insulin-sensitive (IS) and insulin-resistant (IR) cells, upregulated mitochondrial fusion-related genes (MFN1 and OPA1) in IR cells, and improved cellular glucose uptake. Notably, IR cells exhibited greater responsiveness to Mdivi-1 than IS cells, as evidenced by enhanced glucose utilization, elevated ROS generation, increased apoptosis (24.1 *vs.* 18.8 % in IS cells), and increased PI3K expression. Despite improvements in insulin responsiveness, Mdivi-1 adversely impaired mitochondrial function, as demonstrated by reduced ATP production and decreased mitochondrial membrane potential (MMP). These alterations were accompanied by G0/G1 cell-cycle arrest, chromatin condensation, downregulation of mTORC1, and impaired ribosomal biogenesis, with most cells exhibiting single hypertrophic or fragmented nucleoli. **Conclusion**: These findings demonstrate that although Mdivi-1 ameliorated insulin resistance and partially restored insulin signalling, its beneficial effects are accompanied by mitochondrial dysfunction, enhanced apoptosis, and nucleolar alterations. These observations underscore the necessity for therapeutic strategies that selectively restrict mitochondrial fission while preserving mitochondrial integrity and cellular viability.

Keywords

Hyperglycaemia; mitochondrial dynamics; Mdivi-1; diabetes mellites; ribosomal biogenesis

Introduction

Mitochondria change their shape, size, and function to modulate their energy-related performance in relation to different intracellular and extracellular physiological conditions [1]. This dynamic process is tightly regulated by a core set of highly conserved proteins, including the outer mitochondrial membrane (OMM) bound Mitofusin1 (MFN1) and Mitofusin2 (MFN2), together with Optic atrophy 1 (OPA1), which collectively mediate mitochondrial fusion. In parallel, mitochondrial fragmentation involves a large GTPase (dynamin-related protein-1, DRP1) and adaptor proteins, including the mitochondrial fission-1 protein (FIS1) and the

mitochondrial fission factor (MFF). These nuclear-coded proteins are integrated to ensure mitochondrial-related events, including fusion/fission balance, quality control, and redox homeostasis [2]. On the cellular level, dysregulation of mitochondrial dynamics contributes to mitochondrial DNA (mtDNA) depletion, impaired mitochondrial functions, and ultimately cell death. Accumulating evidence further highlighted the role of abnormal mitochondrial dynamics in the pathogenesis of several diseases, including cancer and diabetes mellitus [3]. Previous studies, for example, have suggested a link between hyperglycaemia, a hallmark of diabetes mellitus (DM) and mitochondrial dysfunction [4], due to the downregulation of mitochondrial dynamics-related genes [5,6]. Also, hyperglycaemia enhanced mitochondrial fission in endothelial cells [7], diabetic mice [8] and aged diabetic patients [9,10]. Although the mechanisms underlying these observations remain insufficiently understood, several studies suggested that hyperglycaemia-induced mitochondrial fragmentation is mediated by proteins involved in calcium channels [11] and impaired cellular energy production. Also, the overproduction of reactive oxygen species (ROS) serves an essential role in the genesis of these conditions [1]. Furthermore, some metabolic and physiological changes, such as excessive hepatic glucose production, upregulation of inflammatory proteins, insulin resistance, and impaired glucose tolerance, are predisposing factors for diabetes and its associated complications [12-13].

Despite the pathological consequences associated with impaired mitochondrial dynamics, some studies suggested potential therapeutic strategies of targeting mitochondrial fission using selective DRP1 inhibitors, such as mitochondrial division inhibitor-1 (Mdivi-1), other mitochondrial fission inhibitors, and certain commonly used drugs for metabolic diseases such as obesity, DM, and cardiovascular disorders. This indicates the physiological/pathological roles of mitochondrial fission, its regulation by DRP1, and the interplay between ROS and mitochondrial dynamics in health and metabolic diseases [14,15].
In another context, several studies have demonstrated enhanced ribosomal biogenesis in glomerular epithelial cells (GECs) cultured under hyperglycaemic conditions [16]. Moreover, emerging evidence revealed that ribosomal biogenesis is closely linked to the pathogenesis of DM, as chronic hyperglycaemia dysregulates the mTOR-S6K signalling axis, resulting in aberrant rRNA synthesis and protein translation. This contributes to impaired insulin signalling and β-cell dysfunction [17]. However, the interplay between mitochondrial dynamics, ribosomal biogenesis and nutrient-related pathways has not been adequately investigated.

Despite growing interest in targeting mitochondrial dynamics, the therapeutic efficacy of mitochondrial fission by Mdivi-1in insulin-resistant cells has not been comprehensively investigated. While the drug is broadly identified as an inhibitor of the intrinsic GTPase activity of DRP1 [18], increasing evidence indicates that its DRP1-independent actions include inhibition of the electron transport chain (ETC) complex I [19] and antiproliferative activity in breast cancer cells [20]. This off-target effect raises an additional concern about the associated mitochondrial dysfunction and cell death. Thus, this study was designed to investigate the direct effect of Mdivi-1-mediated inhibition of mitochondrial fission and the associated mitochondrial and nucleolar modulations in insulin-resistant hepatoma cells.

Experimental

Key reagents and chemicals

Mdivi-1 (Cat. No. IM2550) was purchased from Solarbio Life Sciences, Beijing, China. 2`,7`-Dichloro-fluorescin diacetate (DCFDA) (CAS No. 4091-99-0) and (3-(4,5-dimethylthiazol-2-yl)-2,5-diphenyltetrazolium bromide thiazolyl (MTT) (Cat. No. 20395.02) were from Sigma-Aldrich, USA, and SERVA, Germany, respectively. Insulin was from Novo Nordisk, Denmark. Acridine orange (AO) (Cat. No. 10127-02-3) was from Loba Chemie, India; 4',6-diamidino-2-phenylindole (DAPI) (Cat. No. E-IR-R103) from Elabscience, USA, and ethidium bromide (Cat. No. 15585011) was from Applied Biotechnology, Egypt. Mitotracker-Red (Cat. No.

M22425) was purchased from Invitrogen-ThermoScientific, USA. Tris-buffered saline with Tween-20 (TBST, Cat. No. R042) was from G-Biosciences, MO, USA. The glucose kit (REV. NO.: ADL/IFU/GLU/LIQ/R01) was from AGAPPE DIAGNOSTICS LTD., Ernakulam, Kerala, India. Dulbecco's Modified Eagle Medium (DMEM) with high-glucose, L-glutamine, and conventional supplements, including pen/strep, trypsin/EDTA, and FBS, was purchased from Capricorn Scientific, Germany.

Cells and induction of insulin resistance

Hepatoma cells (HepG2) were obtained from NAWAH, Cairo, Egypt, and cultured in complete DMEM medium using standard cell culture methods. Hepatoma cell lines were passaged and maintained at 37 °C and 5 % CO_2 up to the 4th passage. To determine the concentration of insulin required to induce insulin resistance (IR), HepG2 cells were incubated in high-glucose medium containing 0.01, 0.1 or 1 nM insulin. Accordingly, to develop IR, cells were seeded at a density of 1.5×10^4 in a 24-well plate for 48 h. The media were replaced with media that contained 25 mM (4.5 g L^{-1}) glucose and 1 nM insulin for 36 h [21]. In parallel, insulin-sensitive (IS) HepG2 cells were maintained under standard culture conditions in normal glucose DMEM and insulin-free medium. To monitor IR, glucose uptake was assessed by measuring glucose concentration in the culture medium and calculating the difference relative to glucose concentration in the cell-free medium (CFM). To assess the time dependence of glucose uptake by IR cells, HepG2 cells were incubated in high-glucose medium with 1 nM insulin, and glucose consumption was estimated after 24, 48, and 72 h, using the same method and reagents.

Cell metabolic activity assay

The cytotoxicity of Mdivi-1 was assessed by MTT assay [22], where 10,000 cells per well were seeded (in 96-well plates), followed by a 24 h incubation time. Next, the old culture medium was replaced with fresh medium containing different Mdivi-1 concentrations. After incubation for 48 h in a CO_2 incubator, cells were treated with 200 µl of MTT (5 mg ml^{-1} *per* well, diluted in complete DMEM medium for 4 h in a CO_2 incubator. After medium decantation, acidified isopropanol was added, and the absorbance was measured at 630 nm.

Flow cytometry for apoptosis and cell cycle analysis

Cell apoptosis was determined using the Annexin-V/PI kit (Pharmingen, FITC cat. no. 556547BD, BD Biosciences) according to the manufacturer's instructions. In this protocol, cells were harvested after incubation with a suitable volume of pre-warmed solution trypsin/EDTA and centrifugation. After washing with PBS, the cells were kept in the dark for 15 min with 5 µl of Annexin V-FITC and 5 µl of propidium iodide in 100 µl of 1X binding buffer, before being subjected to flow cytometry. For cell cycle analysis, treated cells were harvested, washed, and permeabilized with 70 % ethanol at 4 °C for 2 to 4 h. After ethanol fixation, cells were washed with PBS, treated with ribonuclease, and then incubated with 200 µl of PI (ab14083) (50 µg ml^{-1}) for 30 min in the dark at 25 degrees. The suspension was then filtered through a 40 µm mesh and analysed for cell cycle phases.

In vitro cell migration assay

The potential effect of Mdivi-1 on cells' *in vitro* migration was evaluated using a wound-healing assay. In summary, cells were seeded in a 12-well plate, left overnight to attach, and maintained until they reached subconfluence. Next, a clear scratch was created across the cell monolayer. The cell monolayer was washed, incubated in media containing Mdivi-1, and the cell-free area was imaged and quantified at 24 h and 48 h using ImageJ software (https://imagej.net/ij/).

Nucleus, nucleolus, and mitochondria staining and imaging by fluorescent microscopy

To investigate the effects of Mdivi-1 on cellular aspects, including nuclear, nucleolar, and mitochondrial integrity, fluorescent staining and imaging analysis were performed in Mdivi-1-treated IS and IR cells. Initially, AO/EB staining was performed to evaluate the effects of Mdivi-1 on cell death and the associated nuclear alterations. Mdivi-1-treated cells were stained with 2 µl (100 µg ml^{-1}) of an AO/EB solution. Following 10 min at 37 °C, the cells were photographed by a fluorescence microscope (Zoe BioRad, USA). Nuclear staining with DAPI was performed to assess chromatin alteration. Briefly, 5×10^3 cells per well were seeded in a 96-well plate, and after 24 h of incubation, cells were treated with Mdivi-1 for 48 h. Next, cells were rinsed with PBS, fixed with 3.7 % formaldehyde, and washed with PBS. Subsequently, the cells were treated with DAPI solution for 15 min, after which they were examined under the blue channel. To assess mitochondrial distribution and integrity, Mitotracker-Red was used to stain mitochondria based on mitochondrial membrane potential (MMP). Following treatment, as previously described, the culture media were removed, and cells were incubated with 50 µl of 250 nM Mitotracker-Red for 15 min. Next, the dye-containing medium was replaced with PBS (50 µl), and cells were imaged using the red channel of a fluorescence microscope. To monitor the number and size of nucleoli, we optimized AO/EB and DAPI staining and fluorescent imaging of fixed cells (*unpublished details*) to enhance nucleolar visibility by differential staining.

Assessment of cellular reactive oxygen species

To estimate cellular ROS, 100,000 cells per well were cultured in a 12-well plate and left for 24 h at 5 % CO_2. After 48 h of Mdivi-1 treatment, the drug-containing medium was removed, and cells were washed with DMEM and treated with 10 µM DCFH-DA (0.5 ml/well) for 30 min. After decanting DCFH-DA, cells were washed once with DMEM and twice with PBS. Finally, 0.5 ml of PBS was added/well, and stained cells were examined under the green channel.

Analysis of gene expression by quantitative real-time polymerase chain reaction

The relative gene expression analysis of genes involved in mitochondrial fusion and fission was performed using the QuantStudio-5 system (ThermoFisher Scientific). Initially, total RNA was isolated with an RNA purification kit (Cat No: SN017-0100, GeneDireX Inc, USA), followed by evaluation of RNA concentration and purity. Subsequently, the RNA isolate was used as a template for cDNA synthesis, performed with the EasyScript First-Strand cDNA Synthesis SuperMix kit (Transgen-Biotech, Cat. No: AE301-02, China) according to the manufacturer's instructions. For the subsequent amplification reaction, 2 µl of cDNA at a concentration of 200 ng μl^{-1} was used in 20 µl reaction mixtures containing 2 µl of gene-specific primers (10 pmol μl^{-1}; listed in Table 1) and 10 µl of SYBR Green master mix (SolGent, Cat. No. WF10303001).

Table 1. Sequence of gene-specific primer pairs used in the expression analysis

Gene	Primer sequence*	Accession number
MFN1	For: 5'CAGGAGGAAATTGATGCAGTTTT-3' Rev: 5'GTCAAGATACTCCATCTGTAGCACAGT-3'	NM_033540.3
MFN2	For: 5' TGGACGCTGTAGTGCATGAGATTC-3' Rev :5' TCCTCGGAACACGGTGTCTCG-3'	NM_014874.4
OPA1	For: 5' CTCACCATGTGGCCCTATTT-3' Rev :5' ACGGTACAGCCTTCTTTCAC-3	NM_001354663.2
DRP1	For: 5' GATGCCATAGTTGAAGTGGTGAC-3' Rev 5' CCACAAGCATCAGCAAAGTCTGG-3'	NM_001278464.2
FIS1	For: 5' GAACTACCGGCTCAAGGAATAC-3' Rev :5' CCCACGAGTCCATCTTTCTTC-3'	NM_016068.3
β-ACTIN	For: 5' ATCAAGATCATTGCTCCTCCTG-3' Rev :5' GTCATACTCCTGCTTGCTGAT-3'	NM_001101.5

*For: forward; Rev: reverse

The amplification program included a single denaturation step, followed by 45 repeated cycles of denaturation at 95 °C for 5 seconds, annealing at 60 °C, and extension at 72 °C for 20 seconds. A melting curve analysis was performed at 95 °C to monitor fluorescence changes as double-stranded DNA dissociated into single strands. The housekeeping gene β-actin primers were used for normalization (as a reference gene) against the tested genes. The fold changes were calculated using the $2^{-\Delta\Delta Ct}$ method.

Immunoblotting

To analyse the expression of IRS-1 and PI3K, the Prep™ protein extraction kit was utilized to isolate cellular proteins. Bradford reagent was also used to measure protein concentration. Cell lysate containing 20 µg of protein was added to an equal amount of Laemmli sample buffer and used for western blot analysis. Before loading onto the gel, the resultant solution was heated for 5 min at 95 °C. Following electrophoresis and 1 h for membrane blocking, the membrane was incubated overnight at 4 °C with primary antibodies against IRS-1 and PI3K diluted in TBST. A goat monoclonal antibody (Novus Biologicals) conjugated to HRP (Goat anti-rabbit IgG-HRP, 1 mg) was then applied to the blot for 1 h after the blot had been washed 4 times with TBST. A chemiluminescent substrate was added after additional TBST washing, and the resultant signals were detected and analysed.

Statistical analysis and graphing

Data analysis was executed by GraphPad Prism, Version 9.1.0 (http://www.graphpad.com). Data are graphed as the average of at least 3 experiments (± SD). Statistical differences between means were assessed using two-way analysis of variance (ANOVA) and post hoc Tukey's test. Differences were considered significant at *p*-values <0.05. Moreover, GraphPad Prism was used to present results in graphs and illustrations. In all graphs, bars represent the mean values of 3 measurements. Post hoc Tukey's test was used after the two-way ANOVA test to compare means. *, **, *** and **** refer to p <0.05, p <0.01, p <0.001 and p <0.0001, respectively; ns: not significant.

Results

Developing insulin resistance in hepatoma cells

An insulin-resistant cellular model was established in hepatoma cells (HepG2) by incubating cells in high-glucose medium (25 mM) supplemented with 0.01, 0.1, or 1 nM insulin for 36 h. Morphologically, insulin treatment did not induce any noticeable changes in cell shape or viability (Figures 1A-D). Insulin-sensitive (IS) and insulin-resistant (IR) cells consumed significantly greater amounts of glucose (p <0.0001, 0.0001, respectively) compared to the glucose concentration in cell-free media (CFM); however. IR cells showed a significant reduction in glucose uptake compared to IS cells cultured in regular glucose and insulin-free media (p <0.0001), indicating the development of insulin resistance (Figures 1E and F).

To avoid cell senescence and other effects, the lowest insulin concentration that induces insulin resistance (1 nM) was selected for the subsequent experiments. Also, IR persistence was assessed by incubating IR cells in high-glucose (25 mM) and insulin-containing media for 24, 48, or 72 h. The low rate of glucose uptake was maintained over these periods (Figure 1G).

Effect of mitochondrial division inhibitor on cell viability, metabolic activity and glucose uptake

Next, the direct effect of Mdivi-1 on cells was investigated in various aspects. Initially, Mdivi-1 treatment led to mild apoptotic morphological features, including cell rounding and plate detachment in both IS and IR cells (Figure 2A). Also, cell metabolic activity was assessed using the MTT assay after treatment with a range of Mdivi-1 concentrations (20 to 100 µM) for 48 h. Cell viability decreased progressively and in a concentration-

dependent manner when IS and IR cells were treated with Mdivi-1, with IC50 values of 45.64 and 43.67 µM, respectively (Figures 2B and 2C). Moreover, Mdivi-1 enhanced glucose uptake by both cell types (Figure 2D).

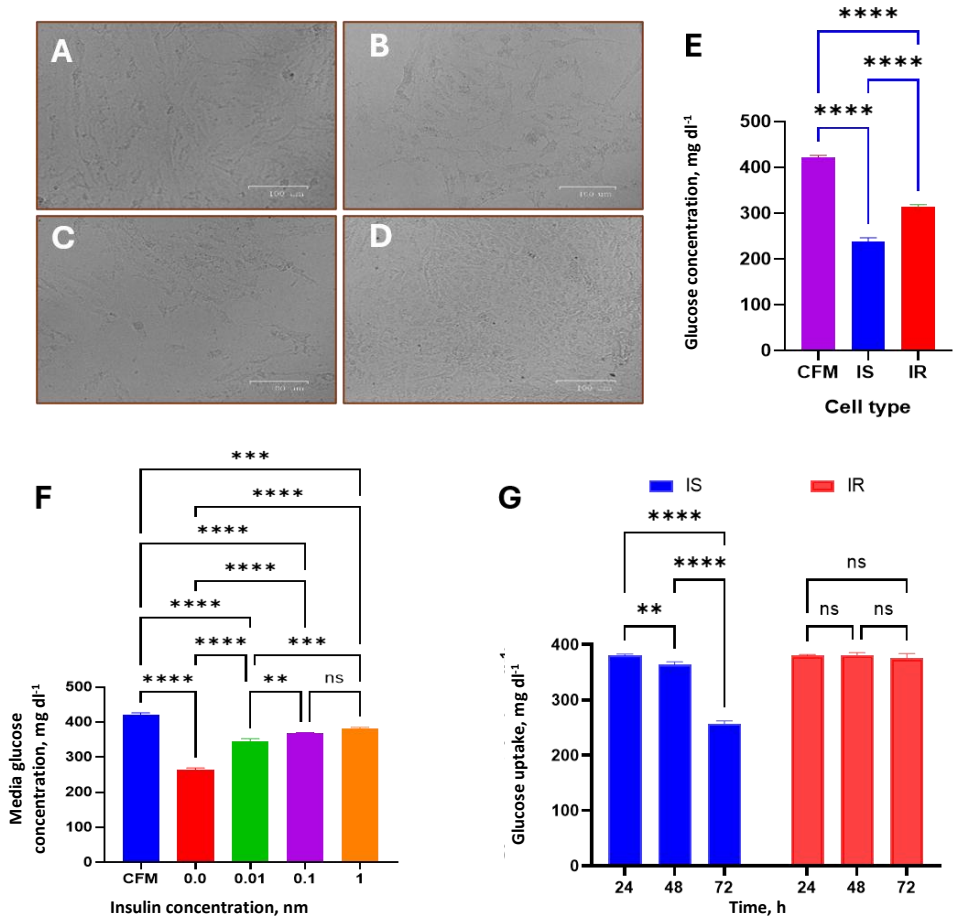

Figure 1. Effect of high glucose and insulin variation on hepatoma cell morphology and glucose uptake. (A) through (D) are representative phase-contrast micrographs of cells incubated in media containing high glucose (4.5 mg ml^{-1}) and 0.0 nM (A). 0.01 nM (B), 0.1 nM (C), and 1 nM (D) insulin. (E) shows the rate of glucose uptake by IS and IR cells, with IR cells consuming significantly less glucose than IS cells and the baseline glucose level measured in cell-free medium (CFM). (F) shows glucose concentration after cells were incubated in high-glucose, insulin-containing medium. (G) Demonstrates the rate of glucose uptake by IR HepG2 cells after 24 h, 48 h, and 72 h under hyperglycaemic conditions and 1 nM insulin

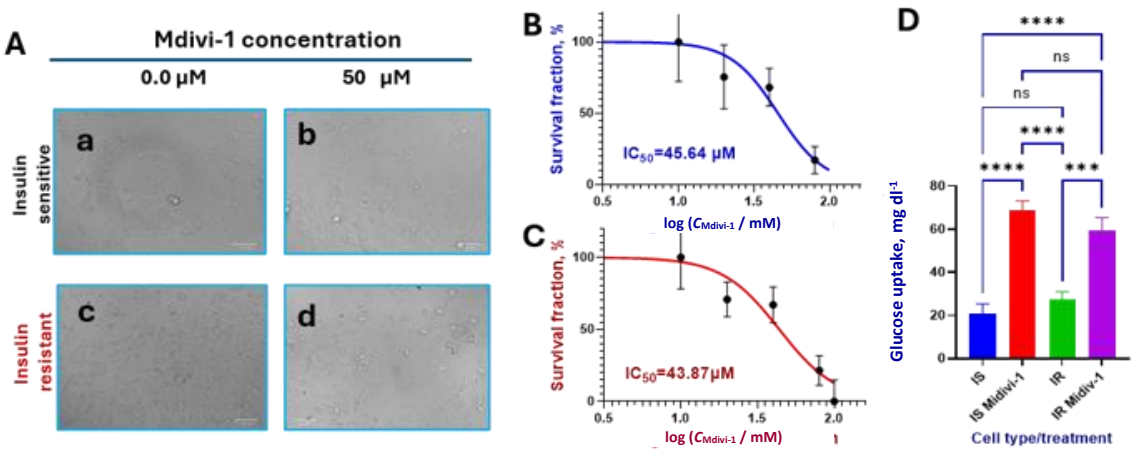

Figure 2. Effect of Mdivi-1 treatment on cell viability and glucose uptake by IS and IR cells. Panel A shows representative phase-contrast micrographs of cells incubated with Mdivi-1-containing media for 48 h, where cells demonstrated mild apoptotic morphological features (b and d). Panels (B) and (C) show the cell viability curve and IC_{50} values of IS and IR cells, respectively. (D) shows the enhanced glucose uptake after treatment with Mdivi-1 for 48 h in both IS and IR cells

To study Mdivi-1 effect on apoptosis-mediated cell death, cells were dually stained with Annexin-V/PI after cells being treated with Mdivi-1, followed by flow cytometry (Figure 3A). We found that Mdivi-1-mediated inhibition of mitochondrial fission induced apoptosis in 18.8 and 24.1 % of IS and IR cells (p <0.0001), respectively (Figure 3B). Moreover, Mdivi-1 effectively arrested 73.7 and 76 % of IS and IR cells, respectively, in the G0/G1 phase (Figures 3C and 3D).

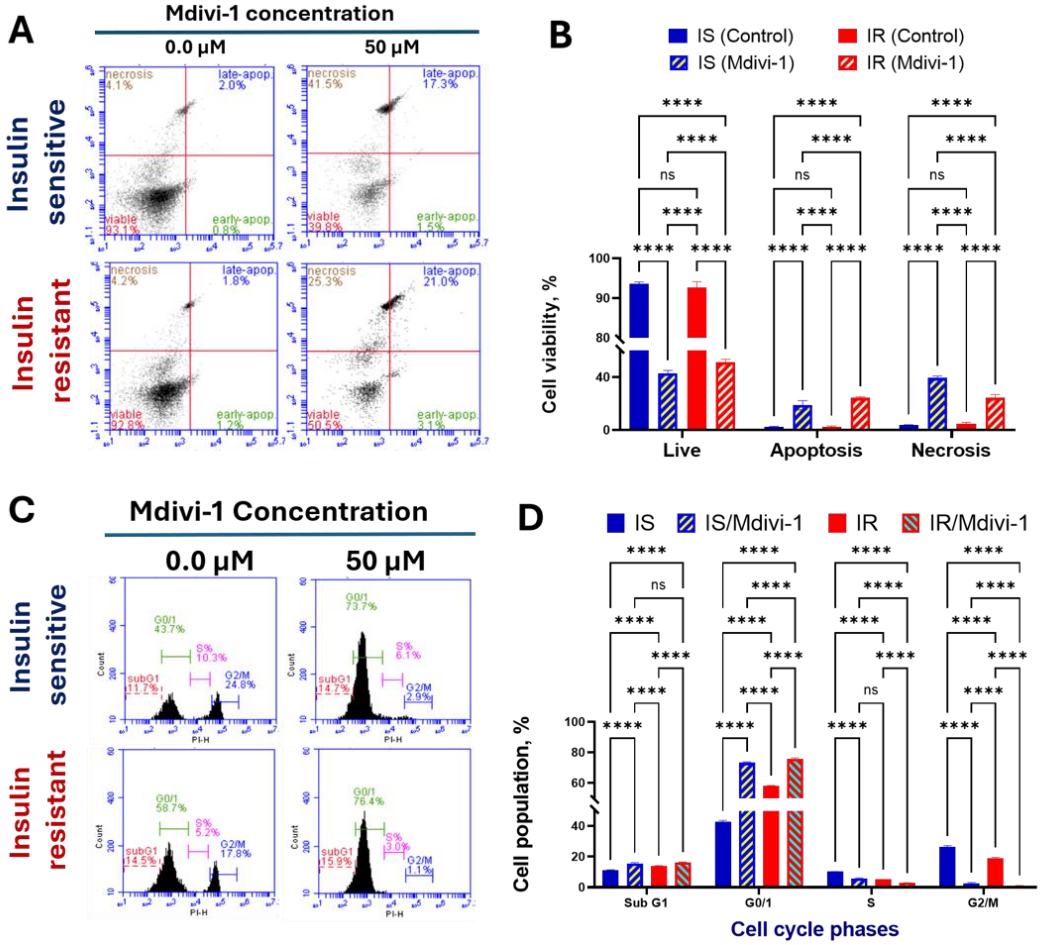

Figure 3. Apoptosis and cell cycle analysis in IS and IR HepG2 cells treated with 50 µM Mdivi-1 for 48 h. Cells were dually stained with Annexin-V/PI /PI and subjected to flow cytometry. Panel (A) includes representative scatter plots, in which each blot's lower-left and lower-right quadrants correspond to viable and early apoptotic cells, respectively. Cells undergoing late apoptosis are found in the upper-right quadrant, and dead cells are in the upper-left quadrant. Bar graph (B) represents a comparative analysis of apoptosis between different treatments. (C) includes representative histograms of cell cycle analysis demonstrating the percentage of cell populations in different cell cycle phases. The bar graph (D) represents the average of three experiments (±SD).

Effect of Mdivi-1 on cell migration, reactive oxygen species production and antioxidant profile

As insulin signalling and Mdivi-1 may affect cell migration, we assessed the migration ability of cells by an *in vitro* wound healing assay, which demonstrated the regression of cell migration in IS and IR cells after being treated with Mdivi-1 for 24 and 48 h compared to the corresponding time point of Mdivi-1-untreated cells (p <0.0001, p <0.0001, respectively) (Figure 4). Additionally, Mdivi-1 treatment significantly enhanced ROS production in both IS and IR cells (p < 0.0001 and p < 0.0001, respectively) (Figures 5A and B). In parallel, ELISA analysis of the antioxidant markers (Nrf2, GSH and SOD) demonstrated that inhibition of mitochondrial division was associated with a significant increase in the concentration of Nrf2 (p <0.001), GSH (p <0.05) and SOD activity (p <0.001) in IR cells relative to the corresponding untreated IR cells (Figures 5C, D and E, respectively). The phenotype role (IS *vs.* IR) was significantly observed in GSH and SOD results.

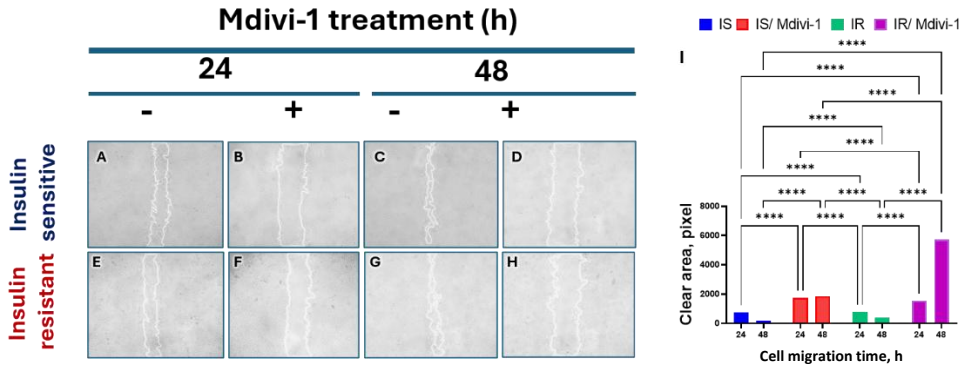

Figure 4. *In vitro* cell migration assay of IS (A-D) and IR (E-H) HepG2 cells after treatment with Mdivi-1 for 24 or 48 h, where Mdivi-1 led to regression of cell migration in both IS and IR cells. The bar graph (I) represents the clear area of different cell populations assessed by ImageJ in pixels

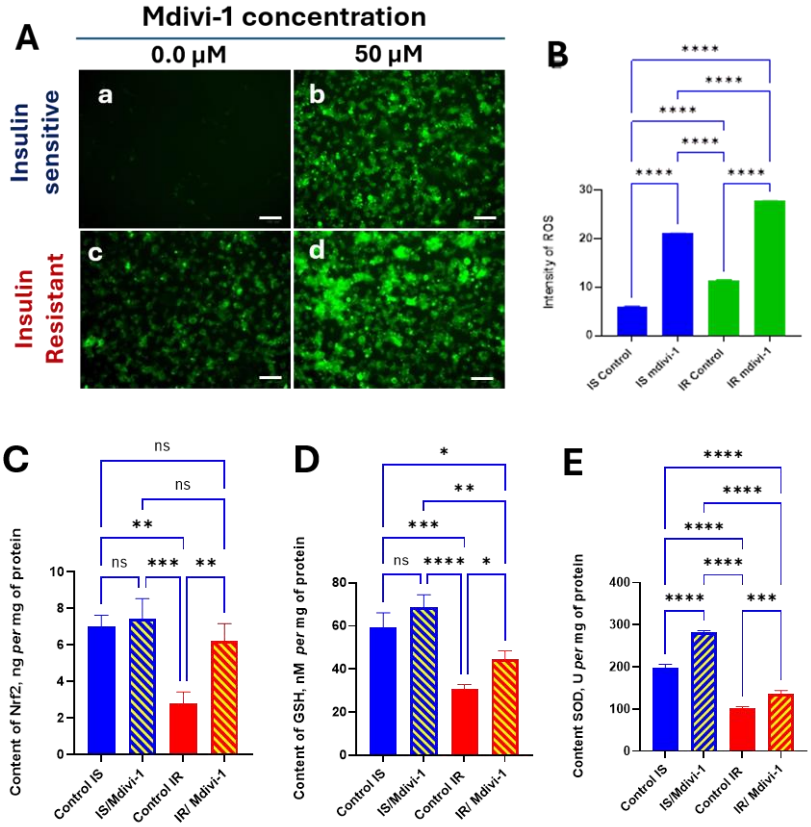

Figure 5. Cellular reactive oxygen species and antioxidant markers in IS and IR cells after being treated with Mdivi-1. Panel (A) includes fluorescent micrographs of cells untreated or treated with 50 µM Mdivi-1 for 48 h, stained with DCFDA, and imaged by a fluorescence microscope (Scale bar: 100 µm). (B) is the integrated density estimated after channel splitting by ImageJ. (C), (D) and (E) show the levels of cellular antioxidant markers Nrf2, GSH and SOD, respectively, determined by ELISA

Nuclear changes and expression of the mitochondrial dynamics-related genes

On the nuclear level, AO/EB dual staining and DAPI demonstrated that Mdivi-1 induced moderate nuclear apoptotic (not necrotic) effects and chromatin condensation, respectively (Figure 6). In parallel, expression analysis at the mRNA or protein levels examined two sets of genes: mitochondrial dynamics-related genes (fusion- and fission-related genes) and insulin-PI3K-AKT/Glut4-mTOR-related genes. In the first set, DRP1 expression was significantly reduced in both IS and IR cells treated with Mdivi-1 compared with their corresponding untreated cells (p <0.0001 and p <0.05, respectively). However, FIS1 decreased only in Mdivi-1-treated IR cells (p <0.0001). In contrast, the mitochondrial fusion-related genes (MFN1 & OPA1) were

upregulated in Mdivi-1-treated IR cells, compared to untreated control cells (p <0.0001, p <0.0001, respectively) or relative to the corresponding IS cells (p <0.001, p <0.001, respectively) (Figures 7A and B).

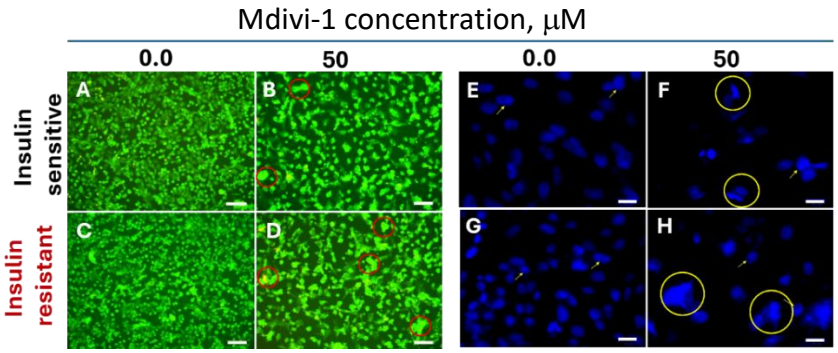

Figure 6. Nuclear changes associated with Mdivi-1 treatment. Fluorescent micrograph of IS and IR HepG2 cells treated with Mdivi-1. A-D are representative fluorescent micrographs of cells dually stained with acridine orange/ethidium bromide (AO/EB) (scale bar: 100 μm). E-H are fluorescent images of cells in which the nuclei were stained with DAPI. Red and yellow circles indicate typical apoptotic cells with distorted nuclear DNA as indicated by chromatin condensation and DNA fragmentation (Scale bar: 50 μm).

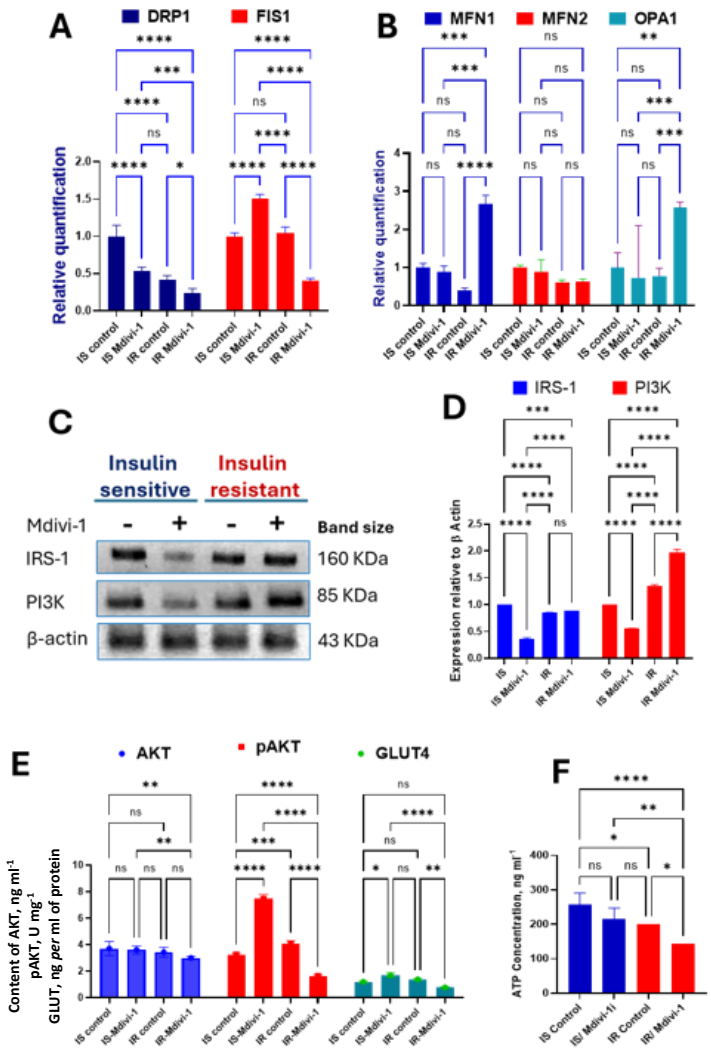

Figure 7. Effects of insulin resistance and DRP1 inhibition on the expression of the mitochondrial dynamics-related genes and PI3K/AKT signalling pathway. Total RNA and proteins were extracted from Mdivi-1-treated IS or IR cells. Messenger RNA was reverse-transcribed to cDNA and used to assess the expression of mitochondrial fission-related genes (DRP1 and Fis1) (A) and mitochondrial fusion-related genes (MFN1, MFN2, and OPA1) (B). (C) and (D) depict the protein expression of IRS-1 and PI3K assessed by immunoblotting. (E) shows the expression of AKT, p-AKT, and GLUT4 expression fold at the mRNA level. (F) shows the level of cellular ATP assessed by ELISA

Assessment of insulin-PI3K-Akt signalling molecules

In parallel, proteins involved in insulin/PI3K/AKT/Glut4 signalling and glucose transporters were assessed by immunoblotting (IRS-1 and PI3K) or ELISA (AKT, pAKT, and Glut4). As shown in Figures 7C and D, Mdivi-1 reduced IRS-1 only in IS cells (p <0.0001); however, it exerted an opposite effect on PI3K and Glut4 levels in IS and IR cells (p <0.0001, p <0.0001, respectively). Although AKT protein was unaffected by insulin resistance or Mdivi-1 treatment, both pAKT and Glut4 were oppositely changed in IS and IR cells, where they were incubated with Mdivi-1 (Figure 7E). Furthermore, ATP generation decreased insignificantly in IS cells ($p > 0.05$), but decreased significantly ($p < 0.05$) when IR cells were treated with the drug (Figure 7F).

Effect of Mdivi-1 on mechanistic target of rapamycin (mTOR) and ribosomal biogenesis

As insulin is a major regulator of the mTOR pathway and protein synthesis, the study aimed to investigate the direct effects of IR and Mdivi-1 on ribosomal biogenesis and the mTOR pathway. This was done by detecting changes in nucleolar number and size, assessed by cell fixation/antibody-free fluorescent imaging. As Figures 8A (a-d) and 9 show, both insulin resistance and Mdivi-1 decreased nucleolar count (per nucleus) as indicated by the increased percentage of cells with a single nucleolus. Additionally, Mdivi-1 reduced the mitochondrial membrane potential (MMP) assessed by the MMP-based mitochondrial staining and fluorescent imaging (Figure 8C). In parallel, both IR and Mdivi-1 decreased the level of mTORC1 (Figure 8D).

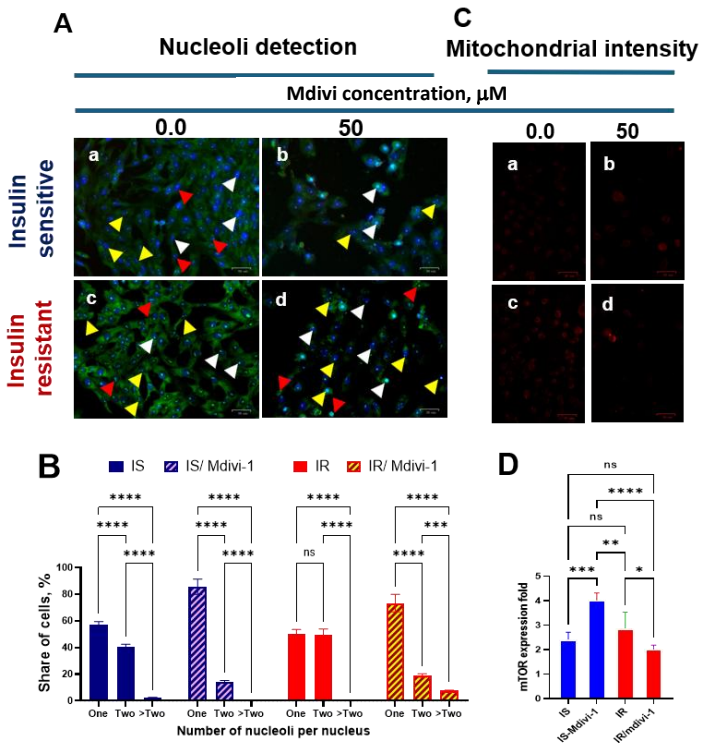

Figure 8. Fluorescent micrographs of nucleoli imaging and the changes in mitochondrial membrane potential (MMP) in IS and IR hepatoma cells after Mdivi-1 treatment. Fluorescent micrographs (A) show the changes in the number and size of the nucleoli in IS cells (a), IS cells pretreated with Mdivi-1 (b), IR cells (c), and IR cells pretreated with Mdivi-1 (d). (B) depicts the share of cells with a single nucleolus, two nucleoli, three, or more nucleoli (white, yellow and red arrows, respectively, in Figure A). Fluorescent images (C: a-d) demonstrate the mitochondrial membrane potential (following a similar order in the nucleoli detection), in which cells were stained with Mitotracker-Red. Scale bar = 50 µm. (D) illustrates the expression of mTORC1 protein assessed by ELISA

Discussion

This work demonstrates that tilting the mitochondrial dynamics balance toward mitochondrial fusion through DRP1 inhibition by Mdivi-1 enhances glucose uptake and IRS-1 expression in IR hepatoma cells,

indicating the attenuation of insulin resistance. However, these antidiabetic improvements were accompanied by detrimental mitochondrial, subnuclear, and cellular alterations. Initially, chronic exposure of hepatoma cells to high glucose and insulin induced insulin resistance, characterised by reduced glucose uptake from culture media, elevated cellular ROS and impaired antioxidant defence system (Nrf2, GSH and SOD). Although Mdivi-1--mediated DRP1 inhibition restored insulin responsiveness *via* promoting mitochondrial fusion and glucose consumption, these effects were accompanied by mitochondrial dysfunction, nuclear alterations, cell cycle arrest, and apoptosis. Moreover, the concurrent suppression of ribosomal biogenesis and pAKT/mTORC1 signalling further suggests that sustained inhibition of mitochondrial fission improves insulin sensitivity at the expense of cellular homeostasis. Notably, the IR cellular model was generated in hepatoma (HepG2) cells as the liver is a crucial organ for the regulation of systemic glucose homeostasis. Also, hepatic insulin resistance is one of the earliest and most important metabolic abnormalities in type 2 diabetes [23]. Moreover, hepatocytes contain the complete insulin signalling pathway and a well-investigated platform for the crosstalk between insulin signalling and other signalling pathways, including gluconeogenesis and mTOR pathways [24]. Additionally, hepatocytes reproduce all metabolic changes observed in DM, such as reduced insulin sensitivity, ROS overproduction, and lipid accumulation [25]. Although HepG2 cells or similar cell lines are not the optimal experimental platform for mimicking the hepatic microenvironment, they exhibit greater responsiveness to resistance and the associated cellular changes [26], including apoptosis, ROS production, and modulation of mitochondrial dynamics-related genes [27].

Our findings demonstrated that IR cells exhibited diminished glucose uptake due to impaired insulin signalling, where cells expressed less IRS-1 than IS cells. This impairs insulin/PI3K/Akt signalling and disturbs the translocation and incorporation of GLUT4-containing vesicles into the plasma membrane [28,29]. Also, the development of IR led to an overproduction of cellular ROS and an impairment of antioxidant markers in the high-glucose medium [30,31].

Next, Mdivi-1 was employed to inhibit DRP1 activity, suppressing excessive mitochondrial fission and promoting mitochondrial fusion [18]. In line with previous studies [32], the data showed that Mdivi-1 reduced DRP1 mRNA expression in both IS and IR cells, while increasing mitochondrial fusion gene expression, including MFN1 and OPA1, in IR cells, indicating a shift in mitochondrial dynamics toward fusion. The inconsistent responses of insulin signalling components to Mdivi-1 may reflect a dissociation between the abundance of upstream signalling proteins (such as IRS-1) and their downstream activation. Specifically, the data revealed that increased expression of IRS-1 and PI3K in IR cells following Mdivi-1 treatment was accompanied by reduced AKT and pAKT. Thus, the drug may enhance the availability of upstream signalling proteins; however, this effect appears insufficient to restore the canonical PI3K/AKT axis, indicating the complexity of the effect of Mdivi-1 on insulin signalling.

To avoid potential DRP1 off-targets of Mdivi-1, cells were exposed to 50 µM, rather than the higher concentrations reported in previous studies [33,34]. Moreover, target prediction analysis (Supplementary material, Figure S1) did not identify any of the insulin signalling proteins as significant targets of Mdivi-1. Despite the antihyperglycemic effect of Mdivi-1, it demonstrated several mitochondrial, nuclear, and cellular undesirable effects, including (i) overproduction of cellular ROS, particularly in IR cells, due to the direct transfer of some electrons to O_2, rather than the ETC complexes [35]. The metabolic changes and activation of NADPH oxidase may participate in hyperglycaemia-associated ROS production [36,37]. Furthermore, the increased synthesis of ROS in IR cells may serve as a signalling molecule in Nrf2 activation via the KEAP1 protein [38,39], leading to increased levels of other antioxidant markers, including GSH and SOD [40]. (ii) Treatment of cells with Mdivi-1 led to *apoptosis and cell cycle* arrest in both IS and IR cells; however, it induced more apoptosis in IR than IS cells but similarly arrested cells in the G0/G1 phase in both cell types.

Although the direct impact of Mdivi-1 on the cell cycle of IR hepatoma cells was not previously addressed, it seems that it is cell-type dependent, as some studies documented the G0/G1 arrest in human neuroblastoma cells [41], G2/M arrest in breast cancer [42], and cholangiocarcinoma cells (CCA) [43]. (iii) Mdivi-1 treatment reduced mitochondrial function (ATP production), particularly in IR cells. (iv) More importantly, Mdivi-1 led to mitochondrial dysfunction as indicated by decreased mitochondrial membrane potential (MMP)-based fluorescent signal when cells were stained with Rosamine. (v) Treatment with Mdivi-1 altered ribosomal biogenesis, as assessed by nucleolar imaging. In this regard, ribosomal biogenesis and subsequent protein synthesis are dependent on the nucleolus' integrity. Nuclear fluorescent imaging revealed that IR exhibited a reduced number of cell nucleoli compared with IS cells. Moreover, both insulin resistance and Mdivi-1 treatment led to changes in nucleolar patterns (Figure 9)**,** with treated cells demonstrating lower ribosomal biogenesis, as indicated by the high percentage of mononucleolous cells, suggesting cell cycle arrest and halting protein synthesis. Accordingly, Mdivi-1-mediated mitochondrial dysfunction, oxidative stress, and decreased ribosomal biogenesis may trigger phosphorylation-mediated degradation of IRS-1 [44]. In the IR context, Mdivi-1 did not affect IRS-1, probably due to the activation of alternative pathways, such as MAPK signalling [45,46], or the involvement of epigenetic factors, such as microRNAs [47,48].

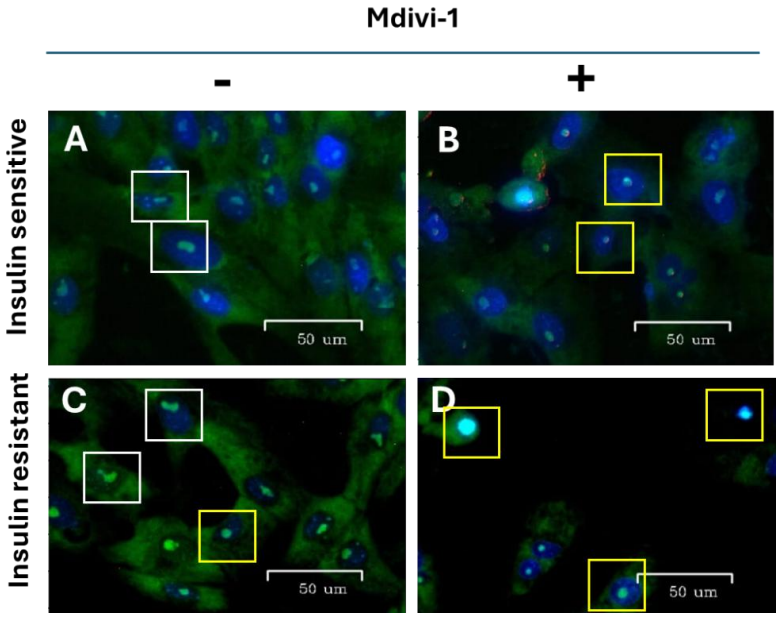

Figure 9. Fluorescent micrographs of paraformaldehyde-fixed and AO/EB/DAPI-stained HepG2 cells (reproduced from Figure 8A) demonstrate changes in the nucleolus count and size. Insulin resistance and/or Mdivi-1 treatment reduced ribosomal biogenesis as indicated by the reduced number of nucleoli/nuclei. White squares refer to nuclei with two or more nucleoli. Yellow squares refer to nuclei with a single nucleolus and a reduced size

Conclusion

In summary, this study highlights the dual effect of Mdivi-1, as it demonstrates a potential to restore insulin sensitivity in insulin-resistant hepatoma cells while exerting antiproliferative effects. In IR cells, the drug downregulated mitochondrial fission genes (DRP1 and FIS1), while upregulating the fusion genes (NFN1 and OPA1). Although Mdivi-1 increased glucose uptake and enhanced PI3K expression in IR cells, the data suggested that it may uncouple glucose uptake from the classical insulin/PI3K/AKT/Glut4 axis. This is supported by Mdivi-1-mediated mitochondrial reprogramming, in which Mdivi-1-mediated inhibition of mitochondrial fission was associated with decreased MMP and ATP, leading to increased cellular demand for glucose independently of AKT activation. This scenario was associated with several cellular and nuclear changes, including apoptosis, dysregulated ribosomal biogenesis, and nutrient-related pathways. These observations may limit the potential nomination of Mdivi-1 as an antidiabetic agent. Further study is needed to distinguish the direct effect of Mdivi-

1 on mitochondrial fission from its role in inhibiting energy-related metabolic function. Although mTORC1 acts as a master regulator linking nutrient availability to ribosome production and protein synthesis, further investigation is needed to clarify the crosstalk between mitochondrial and ribosomal dynamics in insulin-resistant cells.

Supplementary material

Additional data are available at https://pub.iapchem.org/ojs/index.php/admet/article/view/3512, or from the corresponding author on request.

Funding: *This article was generated through research work supported by the Science, Technology& Innovation Funding Authority (STDF) grant ID 48606 and the Egypt-US collaborative project (Grant: C21000152). The work was also partially supported by the ASRT fund (RESPECT 21-9999).*

Acknowledgements: *We acknowledge funding support to Mai H. Soliman through the Postgraduate Support Grant (PGSG) from the Science, Technology & Innovation Funding (STDF) and the Egypt-USA collaborative research fund (Grant ID: C21-000152) to Professor Mohamed Hessien.*

CRediT authorship contribution statement: *M.H. T.D.: Conducted experimental planning, design, and optimization. Conducted fluorescent microscopy and qRT-PCR, edited and reviewed the manuscript. M.H.H.: Is the primary researcher, conducted cell culture-related investigations and performed fluorescent imaging, cell modelling and ELISA experiments. M.H.: is the primary investigator, designed the experimental work, aided in conducting experiments, analysed the results, interpreted data, and edited and reviewed the paper.*

Data availability: *Data are available upon request to the corresponding author.*

Conflict of interest: *Authors indicate no potential conflicts of interest.*

References

[1] S.B. Yu, G. Pekkurnaz. Mechanisms Orchestrating Mitochondrial Dynamics for Energy Homeostasis. *J. Mol. Biol.* **430** (2018) 3922-3941. https://doi.org/10.1016/j.jmb.2018.07.027

[2] S.B. Berman, F.J. Pineda, J.M. Hardwick. Mitochondrial fission and fusion dynamics: the long and short of it. *Cell Death Differ.* **15** (2008) 1147-1152. https://doi.org/10.1038/cdd.2008.57

[3] A.M. Joseph, D.R. Joanisse, R.G. Baillot, D.A. Hood. Mitochondrial dysregulation in the pathogenesis of diabetes: potential for mitochondrial biogenesis-mediated interventions. *Exp. Diabetes Res.* **2012** (2012) 642038. https://doi.org/10.1155/2012/642038

[4] B.B. Lowell, G.I. Shulman. Mitochondrial dysfunction and type 2 diabetes. *Science* **307** (2005) 384-387. https://doi.org/10.1126/science.1104343

[5] S. Rovira-Llopis, C. Bañuls, N. Diaz-Morales, A. Hernandez-Mijares, M. Rocha, V.M. Victor. Mitochondrial dynamics in type 2 diabetes: Pathophysiological implications. *Redox Biol.* **11** (2017) 637-645. https://doi.org/10.1016/j.redox.2017.01.013

[6] G. Twig, A. Elorza, A.J. Molina, H. Mohamed, J.D. Wikstrom, G. Walzer, L. Stiles, S.E. Haigh, S. Katz, G. Las, J. Alroy, M. Wu, B.F. Py, J. Yuan, J.T. Deeney, B.E. Corkey, O.S. Shirihai. Fission and selective fusion govern mitochondrial segregation and elimination by autophagy. *EMBO J.* **27** (2008) 433-446. https://doi.org/10.1038/sj.emboj.7601963

[7] W. Wang, Y. Wang, J. Long, J. Wang, S.B. Haudek, P. Overbeek, B.H. Chang, P.T. Schumacker, F.R. Danesh. Mitochondrial fission triggered by hyperglycemia is mediated by ROCK1 activation in podocytes and endothelial cells. *Cell Metab.* **15** (2012) 186-200. https://doi.org/10.1016/j.cmet.2012.01.009

[8] S. Kumari, L. Anderson, S. Farmer, S.L. Mehta, P.A. Li. Hyperglycemia alters mitochondrial fission and fusion proteins in mice subjected to cerebral ischemia and reperfusion. *Transl. Stroke Res.* **3** (2012) 296-304. https://doi.org/10.1007/s12975-012-0158-9

[9] K.F. Petersen, D. Befroy, S. Dufour, J. Dziura, C. Ariyan, D.L. Rothman, L. DiPietro, G.W. Cline, G.I. Shulman. Mitochondrial dysfunction in the elderly: possible role in insulin resistance. *Science* **300** (2003) 1140-1142. https://doi.org/10.1126/science.1082889

[10] T. Vezza, P. Díaz-Pozo, F. Canet, A.M. de Marañón, Z. Abad-Jiménez, C. García-Gargallo, I. Roldan, E. Solá, C. Bañuls, S. López-Domènech, M. Rocha, V.M. Víctor. The Role of Mitochondrial Dynamic Dysfunction in Age-Associated Type 2 Diabetes. *World J. Mens Health* **40** (2022) 399-411. https://doi.org/10.5534/wjmh.210146

[11] Q.R. Wu, D.L. Zheng, P.M. Liu, H. Yang, L.A. Li, S.J. Kuang, Y.Y. Lai, F. Rao, Y.M. Xue, J.J. Lin, S.X. Liu, C.B. Chen, C.Y. Deng. High glucose induces Drp1-mediated mitochondrial fission via the Orai1 calcium channel to participate in diabetic cardiomyocyte hypertrophy. *Cell Death Dis.* **12** (2021) 216. https://doi.org/10.1038/s41419-021-03502-4

[12] W. Dai, L. Jiang. Dysregulated Mitochondrial Dynamics and Metabolism in Obesity, Diabetes, and Cancer. *Front. Endocrinol.* **10** (2019) 570. https://doi.org/10.3389/fendo.2019.00570

[13] S.M. Shenouda, M.E. Widlansky, K. Chen, G. Xu, M. Holbrook, C.E. Tabit, N.M. Hamburg, A.A. Frame, T.L. Caiano, M.A. Kluge, M.A. Duess, A. Levit, B. Kim, M.L. Hartman, L. Joseph, O.S. Shirihai, J.A. Vita. Altered mitochondrial dynamics contributes to endothelial dysfunction in diabetes mellitus. *Circulation* **124** (2011) 444-453. https://doi.org/10.1161/circulationaha.110.014506

[14] T. Yu, I. Wang, L. Zhang, P.A. Deuster. Mitochondrial Fission as a Therapeutic Target for Metabolic Diseases: Insights into Antioxidant Strategies. *Antioxidants* **12** (2023) 1163. https://doi.org/10.3390/antiox12061163

[15] S.D. Fakhir, I.S. Arif, H.J. Waheed. Dual GLP-1/GIP agonist tirzepatide modulates hepatic mitochondrial fusion–fission gene expression and oxidative stress in diabetic rats. *Pharmacia* **72** (2025) 1-16. https://doi.org/10.3897/pharmacia.72.e175259

[16] M.M. Mariappan, K. D'Silva, M.J. Lee, K. Sataranatarajan, J.L. Barnes, G.G. Choudhury, B.S. Kasinath. Ribosomal biogenesis induction by high glucose requires activation of upstream binding factor in kidney glomerular epithelial cells. *Am. J. Physiol. Renal Physiol.* **300** (2011) F219-F230. https://doi.org/10.1152/ajprenal.00207.2010

[17] L. Jiao, Y. Liu, X.Y. Yu, X. Pan, Y. Zhang, J. Tu, Y.H. Song, Y. Li. Ribosome biogenesis in disease: new players and therapeutic targets. *Signal Transduct. Target. Ther.* **8** (2023) 15. https://doi.org/10.1038/s41392-022-01285-4

[18] Cassidy-Stone, J.E. Chipuk, E. Ingerman, C. Song, C. Yoo, T. Kuwana, M.J. Kurth, J.T. Shaw, J.E. Hinshaw, D.R. Green, J. Nunnari. Chemical inhibition of the mitochondrial division dynamin reveals its role in Bax/Bak-dependent mitochondrial outer membrane permeabilization. *Dev. Cell* **14** (2008) 193-204. https://doi.org/10.1016/j.devcel.2007.11.019

[19] E.A. Bordt, P. Clerc, B.A. Roelofs, A.J. Saladino, L. Tretter, V. Adam-Vizi, E. Cherok, A. Khalil, N. Yadava, S.X. Ge, T.C. Francis, N.W. Kennedy, L.K. Picton, T. Kumar, S. Uppuluri, A.M. Miller, K. Itoh, M. Karbowski, H. Sesaki, R.B. Hill, B.M. Polster. The Putative Drp1 Inhibitor Mdivi-1 Is a Reversible Mitochondrial Complex I Inhibitor that Modulates Reactive Oxygen Species. *Dev. Cell* **40** (2017) 583-594.e6. https://doi.org/10.1016/j.devcel.2017.02.020

[20] A.I. Alalawy, M. Sakran, F.M. Alzuaibr, M.A. Alotaibi, M.E. El-Hefnawy, A.Y. Hazazi, S.M. El-Gendy, E.A. Aidy, H. Effat, D.F. Ismail, M. Hessien. Inhibition of Drp1 orchestrates the responsiveness of breast cancer cells to paclitaxel but insignificantly relieves paclitaxel-related ovarian damage in mice. *Sci. Rep.* **13** (2023) 22782. https://doi.org/10.1038/s41598-023-49578-0

[21] F. Gao, L. Jian, M.I. Zafar, W. Du, Q. Cai, R.A. Shafqat, F. Lu. 4-Hydroxyisoleucine improves insulin resistance in HepG2 cells by decreasing TNF-α and regulating the expression of insulin signal transduction proteins. *Mol. Med. Rep.* **12** (2015) 6555-6560. https://doi.org/10.3892/mmr.2015.4298

[22] F. Denizot, R. Lang. Rapid colorimetric assay for cell growth and survival. Modifications to the tetrazolium dye procedure giving improved sensitivity and reliability. *J. Immunol. Methods* **89** (1986) 271-277. https://doi.org/10.1016/0022-1759(86)90368-6

[23] J.R. Cook, F. Langlet, Y. Kido, D. Accili. Pathogenesis of selective insulin resistance in isolated hepatocytes. *J. Biol. Chem.* **290** (2015) 13972-13980. https://doi.org/10.1074/jbc.M115.638197

[24] R.D. Yudhani, Y. Sari, D.A.A. Nugrahaningsih, E.N. Sholikhah, M. Rochmanti, A.K.R. Purba, H. Khotimah, D. Nugrahenny, M. Mustofa. In Vitro Insulin Resistance Model: A Recent Update. *J. Obes.* **2023** (2023) 1964732. https://doi.org/10.1155/2023/1964732

[25] R.C. Su, A. Lad, J.D. Breidenbach, T.M. Blomquist, W.T. Gunning, P. Dube, A.L. Kleinhenz, D. Malhotra, S.T. Haller, D.J. Kennedy. Hyperglycemia induces key genetic and phenotypic changes in human liver epithelial HepG2 cells which parallel the Leprdb/J mouse model of non-alcoholic fatty liver disease (NAFLD). *PLoS ONE* **14** (2019) e0225604. https://doi.org/10.1371/journal.pone.0225604

[26] V.A. Arzumanian, O.I. Kiseleva, E.V. Poverennaya. The Curious Case of the HepG2 Cell Line: 40 Years of Expertise. *Int. J. Mol. Sci.* **22** (2021) 13135. https://doi.org/10.3390/ijms222313135

[27] D. Shunkina, A. Dakhnevich, E. Shunkin, O. Khaziakhmatova, V. Shupletsova, M. Vulf, A. Komar, E. Kirienkova, L. Litvinova. gp130 Activates Mitochondrial Dynamics for Hepatocyte Survival in a Model of Steatohepatitis. *Biomedicines* **11** (2023) 396. https://doi.org/10.3390/biomedicines11020396

[28] D.E. James, J. Stöckli, M.J. Birnbaum. The aetiology and molecular landscape of insulin resistance. *Nat. Rev. Mol. Cell Biol.* **22** (2021) 751-771. https://doi.org/10.1038/s41580-021-00390-6

[29] S.E. Kahn, R.L. Hull, K.M. Utzschneider. Mechanisms linking obesity to insulin resistance and type 2 diabetes. *Nature* **444** (2006) 840-846. https://doi.org/10.1038/nature05482

[30] I.A. Alvarez, M. Lee, R.S. Eshaq, W. Leskova, N.R. Harris. High Glucose Induces Oxidative Stress That Alters Glycocalyx Proteoglycan Levels in Primary Rat Retinal Microvascular Endothelial Cells and in Isolated Ophthalmic Arteries. *Pathophysiology* **31** (2024) 89-99. https://doi.org/10.3390/pathophysiology31010007

[31] P. Kumar, G.N. Rao, B.B. Pal, A. Pal. Hyperglycemia-induced oxidative stress induces apoptosis by inhibiting PI3-kinase/Akt and ERK1/2 MAPK-mediated signaling pathway causing downregulation of 8-oxoG-DNA glycosylase levels in glial cells. *Int. J. Biochem. Cell Biol.* **53** (2014) 302-319. https://doi.org/10.1016/j.biocel.2014.05.038

[32] M. Manczak, R. Kandimalla, X. Yin, P.H. Reddy. Mitochondrial division inhibitor 1 reduces dynamin-related protein 1 and mitochondrial fission activity. *Hum. Mol. Genet.* **28** (2019) 177-199. https://doi.org/10.1093/hmg/ddy335

[33] M.A. Rogers, J.D. Hutcheson, T. Okui, C. Goettsch, S.A. Singh, A. Halu, F. Schlotter, H. Higashi, L. Wang, M.C. Whelan, A.K. Mlynarchik, A. Daugherty, M. Nomura, M. Aikawa, E. Aikawa. Dynamin-related protein 1 inhibition reduces hepatic PCSK9 secretion. *Cardiovasc. Res.* **117** (2021) 2340-2353. https://doi.org/10.1093/cvr/cvab034

[34] M. Ma, X.H. Lin, H.H. Liu, R. Zhang, R.X. Chen. Suppression of DRP1-mediated mitophagy increases the apoptosis of hepatocellular carcinoma cells in the setting of chemotherapy. *Oncol. Rep.* **43** (2020) 1010-1018. https://doi.org/10.3892/or.2020.7476

[35] R.Z. Zhao, S. Jiang, L. Zhang, Z.B. Yu. Mitochondrial electron transport chain, ROS generation and uncoupling (Review). *Int. J. Mol. Med.* **44** (2019) 3-15. https://doi.org/10.3892/ijmm.2019.4188

[36] T. Nishikawa, D. Edelstein, X.L. Du, S. Yamagishi, T. Matsumura, Y. Kaneda, M.A. Yorek, D. Beebe, P.J. Oates, H.P. Hammes, I. Giardino, M. Brownlee. Normalizing mitochondrial superoxide production blocks three pathways of hyperglycaemic damage. *Nature* **404** (2000) 787-790. https://doi.org/10.1038/35008121

[37] N. Houstis, E.D. Rosen, E.S. Lander. Reactive oxygen species have a causal role in multiple forms of insulin resistance. *Nature* **440** (2006) 944-948. https://doi.org/10.1038/nature04634

[38] Dumas, U.G. Knaus. Raising the 'Good' Oxidants for Immune Protection. *Front. Immunol.* **12** (2021) 698042. https://doi.org/10.3389/fimmu.2021.698042

[39] M. Yamamoto, T.W. Kensler, H. Motohashi. The KEAP1-NRF2 System: a Thiol-Based Sensor-Effector Apparatus for Maintaining Redox Homeostasis. *Physiol. Rev.* **98** (2018) 1169-1203. https://doi.org/10.1152/physrev.00023.2017

[40] H.J. Forman, M. Torres. Reactive oxygen species and cell signaling: respiratory burst in macrophage signaling. *Am. J. Respir. Crit. Care Med.* **166** (2002) S4-S8. https://doi.org/10.1164/rccm.2206007

[41] S.I. Ahn, S.K. Choi, M.J. Kim, J. Wie, J.S. You. Mdivi-1: Effective but complex mitochondrial fission inhibitor. *Biochem. Biophys. Res. Commun.* **710** (2024) 149886. https://doi.org/10.1016/j.bbrc.2024.149886

[42] E. Silva-Pavez, E. Mendoza, P. Morgado-Cáceres, U. Ahumada-Castro, G. Bustos, M. Kangme-Encalada, A.L. de Arbina, A. Puebla-Huerta, F. Muñoz, L. Cereceda, M. Varas-Godoy, Y. Hidalgo, J.C. Cardenas. Mitochondrial division inhibitor (Mdivi-1) induces extracellular matrix (ECM)-detachment of viable breast cancer cells by a DRP1-independent mechanism. *Sci. Rep.* **14** (2024) 14178. https://doi.org/10.1038/s41598-024-64228-9

[43] O. Tusskorn, T. Khunluck, A. Prawan, L. Senggunprai, V. Kukongviriyapan. Mitochondrial division inhibitor-1 potentiates cisplatin-induced apoptosis via the mitochondrial death pathway in cholangiocarcinoma cells. *Biomed. Pharmacother.* **111** (2019) 109-118. https://doi.org/10.1016/j.biopha.2018.12.051

[44] H.F. Jheng, P.J. Tsai, S.M. Guo, L.H. Kuo, C.S. Chang, I.J. Su, C.R. Chang, Y.S. Tsai. Mitochondrial fission contributes to mitochondrial dysfunction and insulin resistance in skeletal muscle. *Mol. Cell. Biol.* **32** (2012) 309-319. https://doi.org/10.1128/mcb.05603-11

[45] Gonzalez-Franquesa, M.E. Patti. Insulin Resistance and Mitochondrial Dysfunction. *Adv. Exp. Med. Biol.* **982** (2017) 465-520. https://doi.org/10.1007/978-3-319-55330-6_25

[46] P. Langlais, Z. Yi, J. Finlayson, M. Luo, R. Mapes, E. De Filippis, C. Meyer, E. Plummer, P. Tongchinsub, M. Mattern, L.J. Mandarino. Global IRS-1 phosphorylation analysis in insulin resistance. *Diabetologia* **54** (2011) 2878-2889. https://doi.org/10.1007/s00125-011-2271-9

[47] H.S. Ryu, S.Y. Park, D. Ma, J. Zhang, W. Lee. The induction of microRNA targeting IRS-1 is involved in the development of insulin resistance under conditions of mitochondrial dysfunction in hepatocytes. *PLoS ONE* **6** (2011) e17343. https://doi.org/10.1371/journal.pone.0017343

[48] P. Sangwung, K.F. Petersen, G.I. Shulman, J.W. Knowles. Mitochondrial Dysfunction, Insulin Resistance, and Potential Genetic Implications. *Endocrinology* **161** (2020) bqaa017. https://doi.org/10.1210/endocr/bqaa017